Hole transport in molecularly doped naphthyl diamine

Tong, K. L.; Tsang, S. W.; Tsung, K. K.; Tse, S. C.; So, S. K.

Published in:
Journal of Applied Physics

DOI:
10.1063/1.2804109

Published: 01/11/2007

Document Version:
Publisher's PDF, also known as Version of record

Hole transport in molecularly doped naphthyl diamine

K. L. Tong, S. W. Tsang, K. K. Tsung, S. C. Tse, and S. K. So[a)]
Department of Physics and Centre for Advanced Luminescence Materials, Hong Kong Baptist University, Kowloon Tong, Hong Kong, China

(Received 3 July 2007; accepted 12 September 2007; published online 6 November 2007)

The effects of dopants on the hole-transporting properties of NPB, i.e., (*N*,*N*′-diphenyl-*N*,*N*′-bis(1-naphthyl)(1,1′-biphenyl)-4,4′ diamine), were studied by time-of-flight technique and admittance spectroscopy. Three dopants were chosen in this study. They were 4-dicyanmethylene-2-methyl-6-4H-pyran (DCM1), rubrene (RB), and tris-(8-hydroxyquinoline) aluminum (Alq_3). It can be shown that DCM1 behaves as hole traps whereas Alq_3 behaves as hole scatterers in NPB. Generally, both trapping and scattering lower hole mobilities in NPB. The hole mobilities decrease when DCM1 and Alq_3 are introduced into NPB whereas the hole mobility remains nearly unchanged when RB is doped into NPB. The effect of doping on carrier dispersion is also studied. © *2007 American Institute of Physics*. [DOI: 10.1063/1.2804109]

I. INTRODUCTION

Organic electronic materials are receiving wide recognition due to their potential applications in electronic and optoelectronic devices. Different devices have been realized. Examples are organic light-emitting diodes (OLEDs), photovoltaic cells, and organic thin film transistors.[1–3] The performances of these device are clearly affected by the charge transporting properties of the organic electronic materials. There are abundant efforts to study charge transports in organic molecules, especially in an amorphous state.[4] Most of these efforts, however, are devoted to the characterization of pristine materials, which are typically unipolar, or sometimes ambipolar. Yet, the optimization of organic devices has gone beyond a single component material in the active layer. In OLED applications, a "cohost" consisting of two charge transporting materials has been used to improve the device lifetimes and luminance efficiencies.[5] Despite the significance of these doped organic materials, measurements of their charge transporting properties are generally lacking. An understanding of the fundamental electrical properties will in turn allow one to improve material design, leading eventually to improved device performance.[6]

This report addresses how dopants affect carrier mobility in NPB, i.e., *N*,*N*′-diphenyl-*N*,*N*′-bis(1-naphthyl)(1,1′-biphenyl)-4,4′ diamine which is widely used as a hole-transporting (HT) material in OLEDs. Besides having chemically stable and excellent film forming abilities, NPB possesses trap-free HT property.[6] Hence, it is an ideal choice for investigating how dopants affect charge transport. Various dopants have been chosen in this study. They are 4-dicyanmethylene-2-methyl-6-4H-pyran (DCM1), rubrene (RB), and tris-(8-hydroxyquinoline) aluminum (Alq_3). Their chemical structures and relevant energy levels are shown in Figs. 1 and 2, respectively. Figure 3 is an illustration depicting how a positively charged hole in NPB is trapped or scattered by dopant molecules as the hole traverses from the left to the right along the direction of an external electric field. As shown in Fig. 2, the highest occupied molecular orbital (HOMO) energy of NPB is about 5.5 eV. When RB or DCM1 is introduced into NPB, hole traps are expected to be introduced [Fig. 3(a)]. If the dopant has a higher-lying HOMO relative to the HOMO of NPB, mobile holes may be trapped by dopant molecules and stop contributing to current flow. On the other hand, if the traps are shallow, trapped carriers may be easily released by thermal energy, resulting in more dispersive time-of-flight (TOF) transients. In this case, the transit time for a carrier increases, as there are trap residing times in addition to the trap-free transit time. When Alq_3 is doped into NPB, positive barriers are built up [Fig. 3(b)]. When holes are in the vicinity of an Alq_3 dopant, carriers may collide with the positive barrier, resulting in hole scattering. The scattering of holes also lengthens transit paths and results in longer transit times.

In this study, TOF technique and admittance spectroscopy (AS) were used to evaluate the hole mobility of NPB.

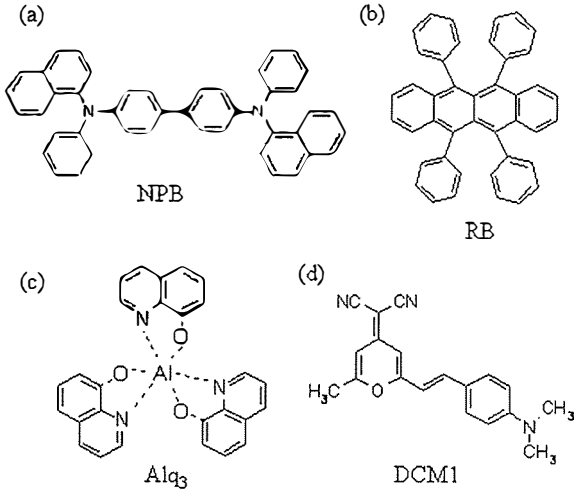

FIG. 1. The chemical structures of (a) NPB, (b) rubrene, (c) Alq_3, and (d) DCM1, where compounds (b)–(d) were used as dopants in this study.

a)Author to whom correspondence should be addressed. Electronic mail: skso@hkbu.edu.hk

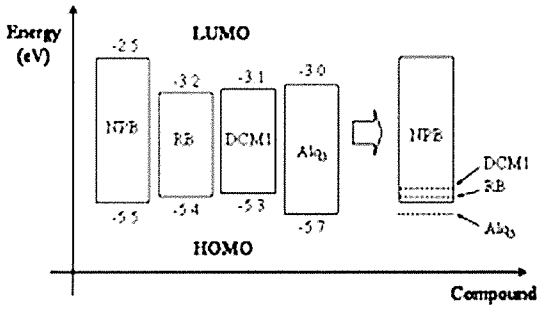

FIG. 2. HOMO and LUMO energy levels of materials used in this study.

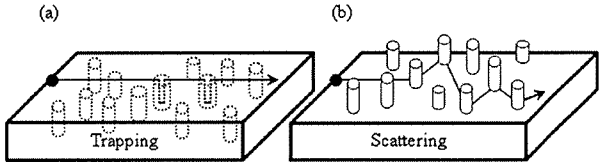

FIG. 3. A schematic diagram depicting how a hole traverses a doped hole-transporting material (host) under the influence of an applied electric field. The field direction points to the right. (a) Hole traps are built up when the dopant has a higher-lying HOMO than the host. (b) Hole scatterers are built up when the dopant has a lower-lying HOMO than the host.

Both experimental techniques require the sample to have a diode structure of anode/organic material/cathode. For TOF, the sample is reverse biased. Free electrical carriers are generated optically by a pulsed uv laser through the cathode, which is semitransparent, if hole mobility determination is needed. Holes are drifted toward the negatively biased anode. The hole transit time then provides a measure of the hole mobility.[7] For AS, free carriers are electrically injected by applying a forward voltage bias to the sample. If hole mobility is needed, the anode should be Ohmic for hole injection while the cathode is electron blocking. The small signal ac impedance (z) of the device is then measured as a function of frequency (f) by applying a small ac modulation superimposed on the dc bias voltage. By measuring the ac response, the complex admittance Y ($\equiv 1/z = i_{ac}/v_{ac}$) can be obtained experimentally. On the other hand, Y can be deduced analytically. Previously, we showed that Y is given by[8]

$$Y(\Omega) = \frac{\varepsilon A}{\tau_{dc} d}\left\{\frac{\Omega^3}{2i[0.75\tilde{\mu}(\Omega)]^2\left[1-\exp\left(\frac{-i4\Omega}{3\mu(\Omega)}\right)\right]+1.5\tilde{\mu}(\Omega)\Omega - i\Omega^2}\right\}, \quad (1)$$

where d and A are the thickness and the area of the sample, respectively. In Eq. (1) above, $i^2=-1$. ε is the permittivity of the organic material. τ_{dc} is the average hole transit time in the absence of the ac signal, and $\Omega = 2\pi f \tau_{dc} = \omega \tau_{dc}$. The normalized mobility is defined as $\tilde{\mu}(\Omega) = \mu(\Omega)/\mu_{dc}$, where $\mu_{dc} = d^2/(V_{dc}\tau_{dc})$ is the dc hole mobility in the absence of the ac field. To extract the carrier mobility, one can analyze the imaginary part of Y in Eq. (1), i.e., the susceptance in the frequency domain. Specifically, the negative differential susceptance of the device can be defined as $-\Delta B \equiv -2\pi f(C - C_{geo})$. By plotting $-\Delta B$ versus f, a maximum at a characteristic frequency $f = \tau_r^{-1}$ can be observed.[9,10] From Eq. (1) and computer simulations, the average carrier transit time τ_{dc} is found to be related to τ_r by[8]

$$\tau_{dc} = 0.56\tau_r. \quad (2)$$

From the known thickness of the organic layer d and the electric field F, the carrier mobility $\mu_{dc} = d/(\tau_{dc}F)$ can be extracted.

II. EXPERIMENT

All organic films were prepared by thermal evaporation under high vacuum conditions on indium tin oxide (ITO) coated glass slides. The coating rate for NPB was 1 nm/s. Doped samples were made by thermal coevaporating NPB with the dopant. Unless stated otherwise, the doping concentration was 1.5% by volume. The samples for TOF had a structure ITO/NPB or NPB-doped layer (7–10 μm)/CuPc (100 nm)/Al (15 nm) where CuPc stands for copper phthalocyanine. A nitrogen pulsed laser (337 nm) was incident through the semitransparent Al electrode. CuPc has a strong optical absorption at 337 nm.[11] As a result, over 90% of the incident uv photons were absorbed within the CuPc layer which effectively acts as a charge generation layer. With the CuPc layer, the hole injection was well defined and effectively independent of the optical absorption of the dopant in NPB.

For AS measurements, Ohmic hole injection contact is required.[8] We used a polymeric conducting anode, poly(3,4-ethylenedioxythiophene) poly(styrenesulfonate) (PEDOT:PSS) as the anode.[12] All AS samples had the structure ITO/PEDOT:PSS (50 nm)/NPB film/Al. The thicknesses of the AS samples were between 3 and 10 μm. The admittance of the sample was evaluated by an impedance analyzer (QuadTech, model 1693 RLC Digibridge). A small ac signal (v_{ac}) with frequency ranging from 12 Hz to 200 kHz was applied on the sample. An external dc voltage (V_{dc}) was simultaneously superimposed on the sample at the same time to test the carrier mobility under different electric fields.

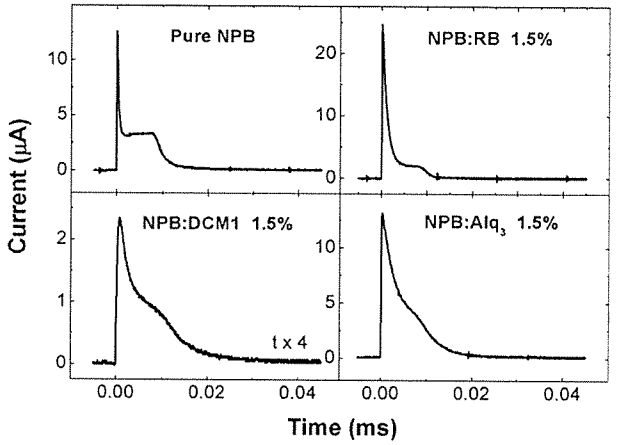

FIG. 4. TOF time transients for NPB, NPB:RB, NPB:DCM1, and NPB:Alq_3 at room temperature under an applied electric field strength of 210 kV/cm.

III. RESULTS AND DISCUSSIONS

Figure 4 shows a set of representative TOF hole transients for pristine NPB and doped NPB at 290 K under an applied electric field F of 210 kV/cm. Clear plateau regions can be observed from the pristine and the RB-doped NPB samples, while more dispersive transients can be observed from the DCM1- and Alq_3-doped NPB samples. From the shapes of the TOF transients, it can be observed that considerable carrier dispersion occurs when DCM1 or Alq_3 is introduced into NPB. The average carrier transit time $\tau_{1/2}$ can be determined from the time for the transient to decay to one-half of the plateau value. The average hole mobility μ_{dc} can be evaluated by $\mu_{dc}=L^2/(V\tau_{1/2})$, where L is the thickness of NPB in the TOF sample and V is the applied voltage. The results are shown as open squares in Fig. 5.

For AS measurements, the raw data consist of a set of

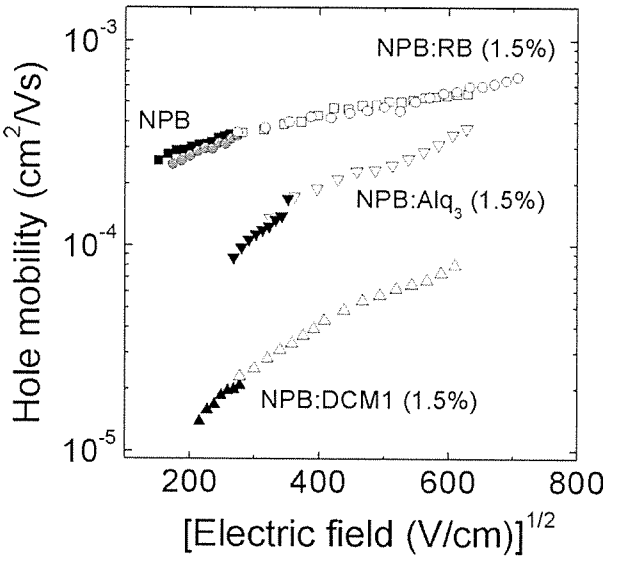

FIG. 5. The hole mobilities of the NPB and the doped NPB samples against the square root of the electric field F at 290 K. The mobilities extracted from TOF are represented by open symbols while those from AS are represented by closed symbols.

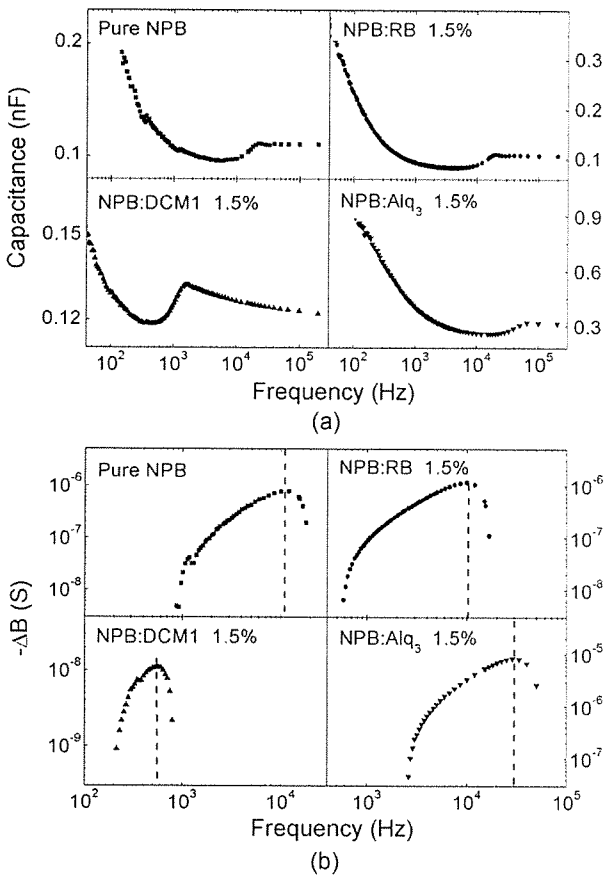

FIG. 6. (a) Capacitances of NPB, NPB:RB, NPB:DCM1, and NPB:Alq_3 at 290 K. The capacitance of the NPB:Alq_3 sample was measured at an applied electric field strength of 115 kV/cm, while the capacitances of other samples were taken at 55 kV/cm. (b) Negative differential susceptance $-\Delta B \equiv -2\pi f(C-C_{geo})$ vs frequency plots as deduced from (a). The vertical dashed lines are locations of frequencies from which average carrier transit times are determined using Eq. (2).

capacitance versus frequency (C-f) plots. Representative data are shown in Fig. 6(a). The capacitances of NPB, NPB:RB, and NPB:DCM1 were captured at an applied electric field strength of 55 kV/cm, while the capacitance of NPB:Alq_3 was taken at 115 kV/cm. Minimum regions of capacitance can be observed at intermediate frequencies for all samples. At high frequency, the capacitances reach steady values, which are equal to their respective geometric capacitances $C_{geo}=\varepsilon A/L$. To extract the average hole mobilities from the AS data shown in Fig. 6(a), we follow the procedures outlined above. From Fig. 6(a), we computed the negative differential susceptance $-\Delta B \equiv -2\pi f(C-C_{geo})$ as a function of frequency f. Then for each case, we plotted the extracted $-\Delta B$ versus f. The results are shown in Fig. 6(b). In each case, a clear maximum in $-\Delta B$ occurs at a well-defined frequency $1/\tau_r$. Using Eq. (2), one can evaluate the average hole mobility. The results are shown as closed symbols in Fig. 5.

From Fig. 5, it can be seen that the hole mobilities obtained independently from TOF and AS are in excellent agreement with each other. The results also suggest that the average carrier transit time, τ_{dc}, as obtained from AS is es-

sentially the same as $\tau_{1/2}$ independently determined from TOF experiments. In general, μ_{dc} varies with the applied electric field F in the form $\mu_{dc} \propto \exp(\beta\sqrt{F})$. β is the Poole-Frenkel slope and is roughly a constant for a particular sample. We note from Fig. 5 that the hole mobility values for the pristine NPB are in excellent agreement with previous reported values and are in the range $(3-6)\times 10^{-4}$ cm^2/V s under the measured field range.[6,13]

Next, we discuss how dopants affect hole mobility in NPB. When RB and DCM1 are introduced into NPB, traps should be formed as suggested by their HOMO offsets with NPB (Fig. 2). In these two cases, both dopants have higher-lying HOMOs relative to that of NPB. However, due to the different HOMO energies of RB and DCM1, the trap depths are different. If we assume that the interaction between the dopant and NPB is weak, then deeper hole traps (~0.2 eV) are expected from DCM1 while shallower traps (~0.1 eV) are expected from RB. As shown in Fig. 5, when DCM1 is doped into NPB, a significant decrease of hole mobility can be observed. The mobility is in the range $(1.5-9)\times 10^{-5}$ cm^2/V s. Compared to the pristine case, a reduction of about 5 times occurs at high field (400 kV/cm) while a much stronger reduction of about 30 times occurs at low field region (40 kV/cm). For RB-doped NPB sample, hole mobilities as deduced from TOF and AS are essentially the same as the pristine NPB sample. The values are in the range $(3-6)\times 10^{-4}$ cm^2/V s. Compared to our previous work, in which doping TPD with RB reduced the hole mobility, the results for this case implied that the HOMOs of NPB and RB are very close to each other.[14,15] The effect of RB doping on the hole transport properties is extremely sensitive to the energy difference between the HOMO level of RB and the host. Therefore, it is conceivable that the difference in HOMO between TPD and RB is larger. Similar observation was obtained from the current-voltage measurement.[16] Finally, for the Alq_3-doped NPB sample, the hole mobility is lowered as compared to the pristine NPB sample. The decrease of mobility can be explained by charge scattering as outlined in Fig. 3. The hole mobility values of Alq_3-doped NPB are in the range $(0.9-4)\times 10^{-4}$ cm^2/V s.

Besides affecting the carrier mobility, doping also affects carrier dispersion. The degree of dispersion of organic materials can be estimated by the tail broadening parameter W defined by[17]

$$W = \frac{\tau_{1/2} - \tau}{\tau_{1/2}} \tag{3}$$

from TOF experimental data. In Eq. (3), τ is the transit time of the leading carriers, and it can be evaluated by the instant at which the TOF signal drops abruptly following the plateau region. The extracted values of W are summarized in Table I. Large W can generally be associated with a high degree of carrier dispersion. As shown in Table I, when DCM1 and Alq_3 are doped into NPB, W increases from 0.13 to 0.24 and 0.20, respectively. The changes of W indicate that the doped NPB samples become more dispersive when compared to the pristine case. It is interesting to notice that when RB is doped into NPB, W decreases to about 0.11. To check whether the reduction is indeed genuine, we repeated the experiment using a RB doping concentration of 3.5%. Again, clear reduction in W to 0.1 can be observed. The precise origin of the improvement in carrier dispersion is not clear. These changes may indicate that the quality of NPB has been improved by RB. This phenomenon may be explained by the similar HOMO levels of NPB and RB. Though NPB behaves as a "trap-free" material, the existence of traps is inevitable. Some intrinsic shallow traps may exist in NPB. So a nondispersive time transients can still be observed for the pure NPB compound. When NPB is doped with RB, those intrinsic traps in NPB may be replaced by the very conducting RB molecules.[18] Thus, the quality of the NPB has been further enhanced. The improvement in the hole conducting properties of NPB by RB doping can, perhaps, shed light on why there is improvement in OLED performance by doping the hole-transporting layer of NPB with RB.[19]

TABLE I. The tail broadening parameter W was obtained from TOF measurements.

	W	σ (meV)	Σ
NPB	0.13	74	1.1
NPB:RB 1.5%	0.11	70	1.0
NPB:DCM 1.5%	0.24	100	1.8
NPB:Alq_3 1.5%	0.20	81	0.8

Apart from room temperature measurements, we also performed temperature dependence of carrier mobilities of the doped films by TOF technique. The data were then analyzed in the framework of the Gaussian disorder model (GDM), first proposed by Bässler.[20] In GDM, charges hop in an amorphous solid whose transport site energies and positions are in Gaussian distributions. The GDM can be embodied in the following semiempirical equation for the carrier mobility:

$$\mu(\hat{\sigma},\Sigma,F) = \mu_\infty \exp\left[-\left(\frac{2\sigma}{3kT}\right)^2\right]\exp\left\{C\left[\left(\frac{\sigma}{kT}\right)^2 - \Sigma^2\right]\sqrt{F}\right\}, \tag{4}$$

where T is the absolute temperature, k is the Boltzmann constant, μ_∞ is the high temperature limit of the mobility, and C is a constant. The energetic disorder σ and the positional disorder Σ can be understood as the width of the Gaussian distribution of the energy states and the position for the transport sites, respectively. Table I summarizes the GDM disorder parameters of the doped NPB from TOF measurements extracted by a procedure outlined before.[16] In the cases of DCM1- and Alq_3-doped NPB, σ increases to 100 and 80 meV, respectively. The increase of σ indicates that the energy levels of DCM1 and Alq_3 broaden the energy distribution of the HOMO. On the other hand, for RB-doped NPB, σ slightly decreases to about 70 meV. The results for this case are not surprising as RB molecules replace some intrinsic traps in NPB.

IV. CONCLUSION

The influence of charge trapping and scattering on charge transport has been studied by doping RB, DCM1, and

Alq_3 into NPB compound. Traps are introduced when NPB is doped with DCM1. The hole mobility decreases from $(3-6)\times10^{-4}$ to $(1.5-9)\times10^{-5}$ cm^2/V s. The reduction of hole mobility for DCM1-doped NPB is due to additional trap residing times, resulting in lower mobility. Scattering also affects hole mobility. When Alq_3 is doped into NPB, the mobility drops from $(3-6)\times10^{-4}$ to $(0.9-4)\times10^{-4}$ cm^2/V s. It can be explained by the increase of the total transit path by carrier scattering. The effect of doping on carrier dispersion was then studied by analyzing the tail broadening parameter W. Both hole scatterer (Alq_3) and trap (DCM1) make NPB more dispersive in hole transport. On the other hand, when RB is doped into NPB, the sample becomes less dispersive.

ACKNOWLEDGMENTS

Support of this research by the Research Grant Council of Hong Kong under Grant HKBU211205E and the Research Committee of Hong Kong Baptist University under Grant FRG/06-07/II-73 is gratefully acknowledged.

[1]C. W. Tang, S. A. VanSlyke, and C. H. Chen, J. Appl. Phys. **65**, 3610 (1989).
[2]C. Brabec, N. Sariciftci, and J. Hummelen, Adv. Funct. Mater. **11**, 15 (2001).
[3]G. Horowitz, J. Mater. Res. **19**, 1946 (2004).
[4]Y. Shirota and H. Kageyama, Chem. Rev. (Washington, D.C.) **107**, 953 (2007).
[5]C. H. Liao, M. T. Lee, C. H. Tsai, and C. H. Chen, Appl. Phys. Lett. **86**, 203507 (2005); H. H. Fong, W. C. H. Choy, K. N. Hui, and Y. J. Liang, *ibid.* **88**, 113510 (2006).
[6]S. C. Tse, K. K. Tsung, and S. K. So, Appl. Phys. Lett. **90**, 213502 (2007).
[7]P. M. Borsenberger and D. S. Weiss, *Organic Photoreceptors for Imaging Systems* (Dekker, New York, 1993), Chap. 9.
[8]S. W. Tsang, S. K. So, and J. B. Xu, J. Appl. Phys. **99**, 013706 (2006).
[9]H. C. F. Martens, H. B. Brom, and P. W. M. Blom, Phys. Rev. B **60**, R8489 (1999).
[10]S. W. Tsang, S. C. Tse, K. L. Tong, and S. K. So, Org. Electron. **7**, 474 (2006).
[11]A. T. Davidson, J. Chem. Phys. **77**, 168 (1982).
[12]S. C. Tse, S. W. Tsang, and S. K. So, J. Appl. Phys. **100**, 063708 (2006).
[13]E. W. Forsythe, M. A. Abkowitz, Y. Gao, and C. W. Tang, J. Vac. Sci. Technol. A **18**, 1869 (2000).
[14]The full name for TPD is *N*,*N*′-diphenyl-*N*,*N*′-bis(3-methylphenyl)(1,1′-biphenyl)-4,4′ diamine.
[15]H. H. Fong, K. C. Lun, and S. K. So, Chem. Phys. Lett. **353**, 407 (2002).
[16]S. K. So, S. C. Tse, and K. L. Tong, J. Disp. Technol. **3**, 225 (2007).
[17]H. H. Fong and S. K. So, J. Appl. Phys. **100**, 094502 (2006).
[18]H. H. Fong, S. K. So, W. Y. Sham, C. F. Lo, Y. S. Wu, and C. H. Chen, Chem. Phys. **298**, 119 (2004).
[19]H. Aziz and Z. D. Popovic, Appl. Phys. Lett. **80**, 2180 (2002).
[20]H. Bässler, Phys. Status Solidi B **175**, 15 (1993).